

Analysis of data concerning smoke control from the 2021 Runehamar full-scale tunnel fire tests

Ying Zhen Li, Haukur Ingason, Lei Jiang, Robert Harley Mostad and Henrik Bygbjerg

RISE Report 2026:37

Financed by TUSC

Analysis of data concerning smoke control from the 2021 Runehamar full-scale tunnel fire tests

Ying Zhen Li, Haukur Ingason, Lei Jiang, Robert Harley
Mostad and Henrik Bygbjerg

Abstract

Data concerning smoke control from full-scale fire experiments conducted in the Runehamar Test Tunnel in Norway in 2021 are summarized and analyzed. The tests were carried out as a part of commercial testing program of high pressure water mist nozzles. These tests included two free-burn tests, and several tests with high pressure water mist based fire suppression systems but only the data prior to activation of the systems are of concern in this study. The data are compared with the established prediction model and demonstrate good consistency. Suggestion on future testing is also made.

Key words: tunnel fire, flow, critical velocity, backlayering length, controlled, uncontrolled

RISE Research Institutes of Sweden
RISE Report 2026:37
ISBN 978-91-90109-66-3
ISSN 0284-5172
Borås 2026

Table of Contents

| | |
|--|-----------|
| Abstract | 3 |
| Table of Contents | 4 |
| Preface | 5 |
| Summary | 6 |
| 1 Introduction | 7 |
| 2 Theoretical background | 8 |
| 3 Test set up | 9 |
| 3.1 Test tunnel | 9 |
| 3.2 Ventilation..... | 10 |
| 3.3 Fire source | 10 |
| 3.4 Blockages in the tunnel | 11 |
| 3.5 Measurements..... | 12 |
| 4 Summary of tests of interest to this study | 14 |
| 5 Analysis of test data | 15 |
| 5.1 Free burn tests 1 and 2..... | 15 |
| 5.1.1 HRR..... | 15 |
| 5.1.2 Smoke control | 16 |
| 5.2 Other tests prior to water spray activation..... | 17 |
| 6 Conclusion | 20 |
| References | 21 |
| Appendix – Measurements at different cross sections | 22 |

Preface

The project is funded by the Tunnel and Underground Safety Center (TUSC), which is greatly acknowledged. TUSC is a research platform for fire safety in underground constructions. The partners are RISE, Swedish Transport Administration, Swedish Fortifications Agency, SKB - the Swedish Nuclear Fuel and Waste Management Company, and Swemin's Health and Safety Committee (GRAMKO).

The full-scale tests were a part of commercial testing of a high-pressure water mist system from Siemens A/S and carried out by RISE Fire Research AS in Norway. Thanks to Henrik Bygbjerg at Siemens for providing the research group with access to the smoke control data and the colleagues at RISE Fire Research in Norway who performed the tests.

Summary

Data from two free-burn tests were analyzed, as well as data from the first 2 mins of five other tests. The data from the free-burn tests are relatively stable, and these tests provide data that support previous prediction models for critical velocity. The differences between the upstream velocities and downstream velocities were found to be small during the relatively stable periods.

The other five tests were designed to test the performance of a high pressure water mist spray system so only the data prior to its activation were analyzed here. Both the fire and the flow are highly transient making it hard to analysis. The scenarios are definitely not quasi-steady but it was possible to give a range of results. It is generally believed that, for a given velocity, if the test was prolonged, the backlayering length would be slightly longer. Furthermore, the differences between the upstream velocities and downstream velocities were found to be more significant here compared to the stable tests. This could be attributed to the transient behaviour of fire and smoke (hot gas expansion related to the larger fire size) and partially to the measurement errors. It is recommended that tests to validate critical velocity correlations should be designed to be quasi-steady to obtain high-quality data. The critical velocities were obtained by inversely calculating from the backlayering data, and as that was highly transient the results had to be given as a range of data.

The blockage ratio close to the upstream edge of the fire source is within 4% - 5%. The blockage ratio from the upstream edge of the fire source to 25 m upstream is about 2%. Further upstream section of interest to this study, the blockage is negligible. Overall, the influences of the blockages are considered small and the data for smoke control have not been corrected using the blockage ratios. If corrections using blockage ratios were done, the data would be slightly higher.

The method of inverse calculations of critical velocity using the confinement velocity with relatively short backlayering was found to work well, and is necessary in order to determine the critical velocity in such type of highly transient tests. In more steady-state tests the method is expected to work better.

1 Introduction

There has been a long-standing discussion about critical velocity and backlayering within the standardization and research community. Much of the data that forms the basis for the calculation models used is based on model experiments. They are also based on a limited number of full-scale experiments, including the Memorial experiments and the Runehamar experiment in 2003. Experiments financed by TUSC have been carried out during the period 2018-2022 (scale 1:3 and 1:15) that relate to critical velocity and backlayering. They are reported separately in reports and articles. Part of the criticism that has been leveled against these theoretical models is that they are largely based on model experiments and that there is a lack of more full-scale experiments for validation of calculations, both at model scale but also for FDS (numerical) calculations. Therefore, there is a great need for more full-scale data, but conducting completely new experiments will require a lot of resources.

There was an opportunity to access data from full-scale water mist experiments conducted in the Runehamar tunnel by RISE Fire Research AS in Trondheim, Norway, in 2021 on behalf of Siemens A/S. The data contained information on backlayering lengths and different air speeds with free-burning experiments with liquid fires, with nominal Heat Release Rates (HRRs) of 7 MW and 30 MW, respectively. There were also experiments where the water mist system is activated after a given time and the information available on backlayering up to activation is of value for the analysis presented here.

There are also full-scale experiments from 2013 and 2016 conducted by RISE Fire and Safety in Borås that need to be analyzed regarding what happened before activation of the fire suppression system (BBS). This will not be done here, but may well be done in near future. By adding more full-scale data to the discussion on critical air speed and backlayering, the goal is to contribute to more verified knowledge in this controversial area.

The objective of this work is to use full-scale data on backlayering and critical air speed from experiments with extinguishing systems and compare with current calculation models.

2 Theoretical background

In the case of no blockage, the critical velocity for smoke control in a tunnel could be estimated using the following correlation [1, 2]:

$$u_c^* = \frac{u_c}{\sqrt{gH}} = \begin{cases} 0.81(Q^*\varphi^{-1/4})^{1/3} & Q^*\varphi^{-1/4} \leq 0.15 \\ 0.43 & Q^*\varphi^{-1/4} > 0.15 \end{cases} \quad (1)$$

where

$$Q^* = \frac{Q}{\rho_o c_p T_o g^{1/2} H^{5/2}}, \quad \varphi = \frac{W}{H}$$

The backlayering length in a tunnel without blockage could be estimated by [1, 3]:

$$L_b^* = \frac{L_b}{H} = 20 \ln\left(\frac{u_c}{u_o}\right) \quad (2)$$

where Q is heat release rate (kW), u_c is critical velocity in a free tunnel (m/s), u_o is longitudinal tunnel velocity in the free tunnel area without blockage (m/s) ($u_o < u_c$), g is gravitational acceleration (m/s^2), L_b is backlayering length (m), c_p is specific heat of air ($\text{kJ/kg}\cdot\text{K}$), T_o is ambient temperature (K), H is tunnel height (m), φ is tunnel aspect ratio (W/H), and ρ_o is ambient air density (kg/m^3). Superscript * refers to dimensionless terms. Note that Eq. (2) can also be written as $u_o/u_c = e^{-0.05L_b/H}$. The above correlations will be used for comparison in the result analysis and thus presented here. They have been widely used and verified to a large extent using both experimental data and numerical results. See for example Gannouni and Maad [4], Hong et al.[5], Weng et al.[6, 7] and Zhang et al.[8].

In case of upstream blockage, the critical velocity usually becomes lower and can be predicted using the correlation based on the blockage ratio [3].

3 Test set up

3.1 Test tunnel

The Runehammar Test Tunnel belongs to the Norwegian Road Administration (NPRA) and was previously a part of the road infrastructure. It is located outside Åndalsnes, Norway, and is a two-way asphalted road tunnel with an approximate length of 1.6 km. The test tunnel is equipped with electricity and facilities for personnel outside the tunnel, and is continuously maintained by the owner NPRA. To provide a site for fire tests, an 80 m long section of the tunnel is protected by fire resistant concrete. See Table 1 for more detailed information on the tunnel. A sketch of the tunnel is shown in Figure 1 and an elevation diagram in Figure 2. A cross-section of the tunnel is shown in Figure 3. The fire source was placed in a nearly flat section.

Table 1. Information on Runehammar Test tunnel.

| Name | Owner | Type (tunnel profile) | Width | Height | Length | Slope |
|------------------------|-------------------------------|----------------------------|---------|---------|------------|-----------|
| Runehammar Test tunnel | Norwegian Road Administration | E 80 (Norwegian Road Norm) | Ca. 9 m | Ca. 6 m | Ca. 1520 m | 1 % - 3 % |

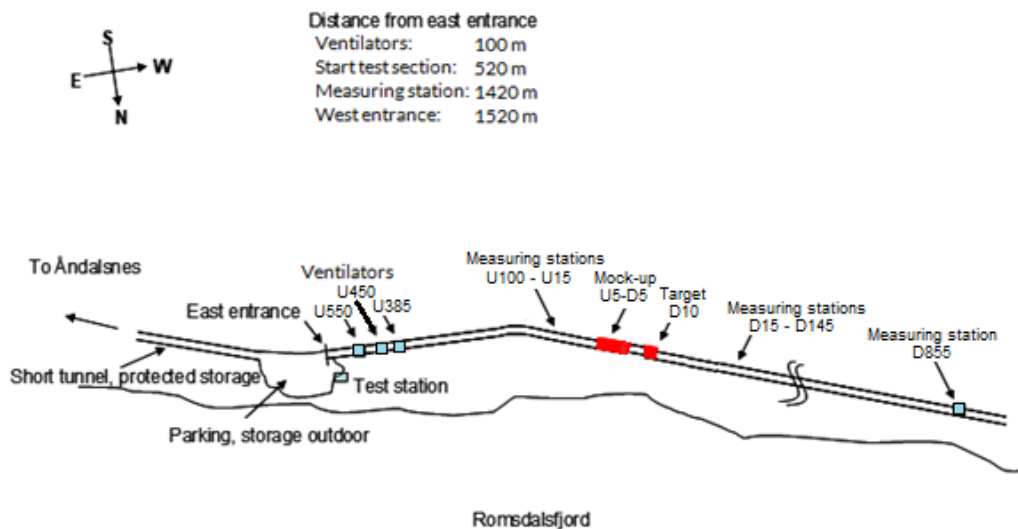


Figure 1 Sketch of the Runehammar Test Tunnel.

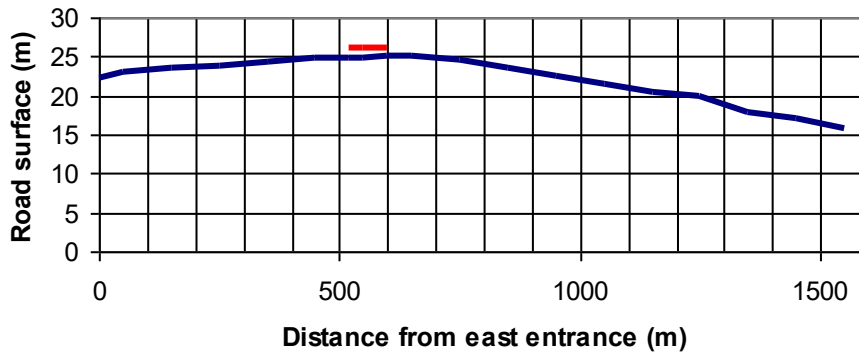


Figure 2 Elevation of the road surface of the tunnel in meters above sea level. The red line indicate the fire zone in the tunnel.

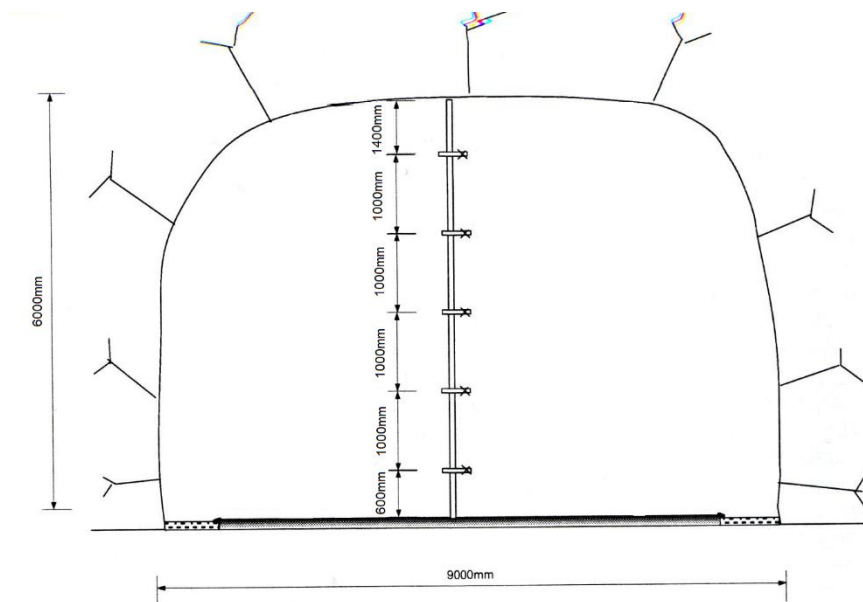


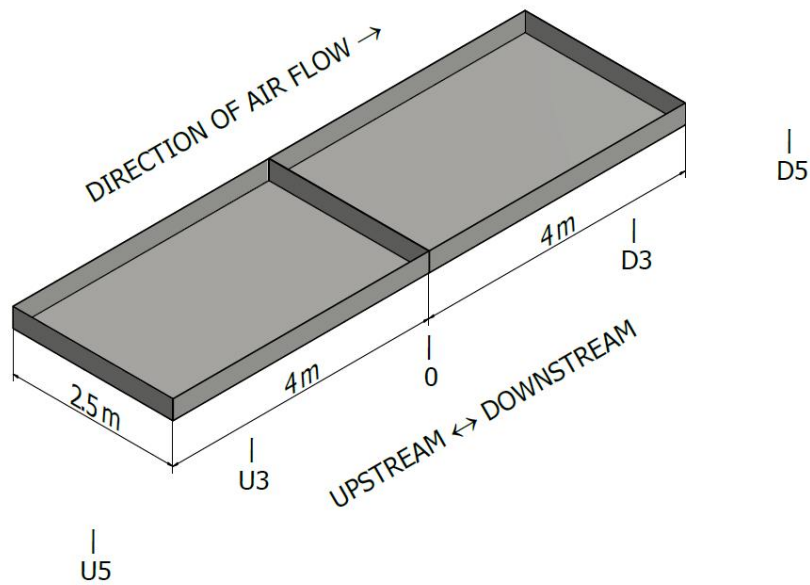
Figure 3 Cross-section of the tunnel, showing the positions of some of the measuring points.

3.2 Ventilation

Five fans are located at 550 m, 450 m and 385 m upstream of the fire, namely U550, U450 and U385. They produced relatively stable air flows near the mock-up.

3.3 Fire source

The fire source was placed at about 600 m from the west portal. In most of tests (tests 3-12), two large pools fitted together, each having dimensions of $2.5 \text{ m} \times 4 \text{ m}$, were used as the fire source, as shown in Figure 4. The two large pools fitted together were filled with 23 mm commercial diesel on a base of 60 mm water. The ignition of the pools was done with a small amount of heptane (1 litre for each pool) to ensure that fuels across the pools were ignited within a short time, less than 60 s. The two pools were ignited simultaneously. The pool fire mock-up was positioned eccentric relative to the centre line of the tunnel. The distance from the side wall to the mock-up was maximum 1.5 m, so one edge of the pools is close to the centerline of the tunnel.



(a) dimensions of the two large pools



(b) a photo of the two large pools

Figure 4 Pools used for tests 3-12.

In the two free-burn tests (test 1 and test 2), different pools were used. The centers of the fire sources were always kept at $x=0$ m. They were positioned along the centerline of the tunnel cross section. In test 1, a 2.56 m^2 ($1.6 \text{ m} \times 1.6 \text{ m}$) pool containing diesel on a water base was used. In test 2, a 15.0 m^2 ($3.2 \text{ m} \times 4.7 \text{ m}$) pool containing diesel on a water base was used, with the longer side across the tunnel width. To facilitate the ignition, 0.5 liter of heptane was poured into the pan in test 1, and 1 litre of heptane was poured in test 2. The fuel was about 90 literes and 200 liters of diesel, respectively.

3.4 Blockages in the tunnel

At 855 m downstream of the fire location, there was a steel container where measurement equipment was stored. This container had approximate dimensions of 1.8 m × 1.8 m. The blockage ratio is estimated to be about 6.8 %. This affects the flow measurement at 855 m and it needs thus to be corrected, i.e., the measured velocities are higher and thus needs to be multiplied by a correction factor which is lower than 1 (0.932 in this case).

On the upstream side of the fire source, there were some concrete blocks along the side walls. The estimated projected area is about 1 m². The blockage of sprinkler pipe is estimated to be around 0.3 m². The blockage of fire source itself is within 0.5 m² - 1 m². There was also a vertical pipe close to the upstream edge of the pools. The blockage ratio close to the upstream edge of the fire source is within 4% - 5%. The blockage ratio from the upstream edge of the fire source to 25 m upstream is about 2%. Further upstream section of interest to this study, the blockage is negligible. Overall, the blockage ratio is kept at a small value to avoid affecting the test results. They are not further considered in this study, but if needed the values presented in this work can be easily converted.

3.5 Measurements

The following was measured during the fire testing:

- Temperatures
- Air velocity
- Oxygen (O₂) concentrations
- Carbon monoxide (CO) concentrations
- Carbon dioxide (CO₂) concentrations
- Humidity
- Visibility
- Heat flux

The locations of the instrumentations are given in Table 2. D = downstream, U = upstream measured from center of the mock-up. The digit in the first column after indicated the distance (in metres) to the center of the fire load. Detailed measurements at different cross sections can also be found in the Appendix.

Light bars were installed at certain locations in the tunnel (e.g., ±35 m and +855 m) to facilitate the installation and observation.

The tunnel longitudinal velocity, u_o , referring to the longitudinal bulk velocity at ambient conditions, was measured at 855 m downstream of the fire source center, using both bi-directional probes and an ultrasonic anemometer. At 100 m upstream, an ultrasonic anemometer was placed along the centreline of the tunnel. The ultrasonic anemometers used were Gill WindObserver II. The accuracy is ±2% at 12 m/s, and the resolution is 0.01 m/s.

The tunnel longitudinal velocity measured at 855 m downstream using the bi-directional probes was corrected based on the blockage ratio as follows:

$$u_o = \frac{C_d C_b \sum (\rho u A_i)}{\rho_o A} \quad (3)$$

In the above equation, ρ is gas density, u is gas velocity, A is tunnel cross sectional area, C_d is the flow coefficient which is 0.817, and C_b is the blockage correction factor that is lower than 1 (0.932 in this case). Subscript i refers to the i th section.

As the measurements started about 30 min prior to ignition, velocity data from the three measurements were obtained. In general, they show very consistent results, both on upstream and downstream side.

Heat release rates were calculated using the oxygen consumption method [9]. The tunnel velocity for heat release rate calculations was estimated based on the flow measurements at 855 m downstream of the fire. Alternatively, the HRRs were calculated using the maximum temperature method, using the correlation proposed by Li and Ingason [10, 11] with the aid of the measured maximum ceiling gas temperatures and the measured velocity. The reason was that for small HRRs, the oxygen sensors were not so sensitive.

Table 2. Simplified diagram of the instrumentation in the tunnel during the fire testing. The heading of each column represent a specific cross-section of the tunnel. Each color and notation represents a specific measurement, e.g. temperature. The heading of each row at the left hand side represent the given height of the cross-section. See description below for explanation of the colored notations, and section 3.1 for more detailed information on each cross section.

| Height [m] | U100 | U50 | U25 | U15 | U5 | U3 | D3 | D5 | D10 | D15 | D25 | D35 | D50 | D100 | D145 | D855 | | | |
|------------|------------|-----|-----|-----|---------|----|----|----|--------|--------------|-----|-----|-----|------|------|------|----|----|----|
| | ← Upstream | | | | Mock-up | | | | Target | Downstream → | | | | | | | | | |
| 6.0 | | | | | TC | TC | TC | TC | TC | | | | | | | | | | |
| 5.0 | | | | | | TC | TC | TC | TC | | | | | | | | | | |
| 4.6 | TC | TC | BP | TC | TC | | | | | | TC | TC | | TC | TC | TC | TC | BP | |
| 4.0 | | | | | TC | TC | TC | TC | TC | | | | | | | | | | |
| 3.6 | TC | TC | BP | TC | TC | TC | TC | TC | TC | TC | TC | TC | TC | | TC | TC | TC | TC | BP |
| 3.0 | | | | | | | | | | | | | | | | | | | |
| 2.6 | TC | TC | BP | TC | TC | | | | TC | TC | TC | TC | | TC | TC | TC | TC | TC | BP |
| 2.5 | | | HU | | | | | | | | | | | | | HU | HU | | |
| 2.0 | US | GA | | | | | | | | | | | | | | GA | GA | | |
| 1.8 | | CM | | HF | | | | | | HF | | HF | CM | | | CM | CM | US | |
| 1.6 | TC | TC | BP | TC | TC | TC | TC | TC | TC | TC | TC | TC | TC | TC | TC | TC | TC | TC | BP |
| 1.5 | | | | | TC | TC | | | | | | | | | | | | | |
| 1.0 | | | | | | | | | | | | | | | | | | | |
| 0.6 | TC | TC | BP | TC | PT | TC | | | | | TC | TC | PT | | TC | TC | TC | TC | BP |

| Notation | Description |
|----------|-------------------------|
| TC | Thermocouple |
| BP | Bidirectional probe |
| GA | Gas analyses |
| HU | Humidity |
| CM | Camera |
| HF | Heat flux meter |
| US | Ultrasonic air velocity |
| PT | Pressure transducer |

4 Summary of tests of interest to this study

The tests of interest to this study are summarized in Table 3. In free burn tests 1 and 2, special pans were used, and the high pressure water mist spray system was not activated. These two tests are of most interest for this analysis. They produced HRRs of about 7.5 MW and 30 MW, respectively. In other tests, the two large pools adjacent to each other were used as the fire source, and the water spray system was activated at 2 min. Therefore, only the smoke spread during the first 2 min prior to the activation of the water spray system is of interest in this study.

During the full-scale fire tests, the tunnel gas temperature is close to the outside temperature which is in a range of 5 to 10 °C. The initial velocity was in a range of 1.4 m/s to 3 m/s. During all of the tests, the backlayering phenomenon was observed at the early stages.

Table 3. A summary of tests of interest to this study.

| Test name | Fuel | Pool dimension | Nr of pools | Initial velocity m/s |
|-----------|--------|----------------|-------------|-------------------------|
| Test 1 | diesel | 1.6 m×1.6 m | 1 | 3 |
| Test 2 | diesel | 6.25 m×2.4 m | 1 | 2.6 |
| Test 3 | diesel | 2.5 m×4.0 m | 2 | 2.5 |
| Test 4 | diesel | 2.5 m×4.0 m | 2 | 1.4 |
| Test 5 | diesel | 2.5 m×4.0 m | 2 | 3 |
| Test 9 | diesel | 2.5 m×4.0 m | 2 | 2.5 |
| Test 10 | diesel | 2.5 m×4.0 m | 2 | 2.4 |
| Test 12 | diesel | 2.5 m×4.0 m | 2 | 2.3 |

5 Analysis of test data

5.1 Free burn tests 1 and 2

5.1.1 HRR

See Figure 5 and Figure 6 for HRR calculations during the calibration tests. By default, HRRs were calculated using the oxygen method. However, in Test 1, the gas analysers were only functioning during a short period. Therefore, the alternative method for calculating HRRs using the maximum temperature (MT) method [10, 11] was also used. In general, the HRRs based on the two different methods are consistent.

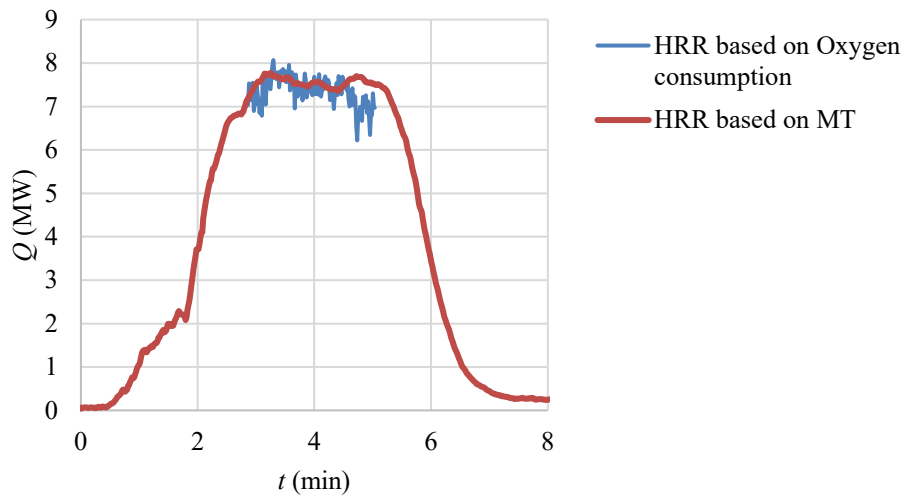


Figure 5 HRR curve calculated for Test 1.

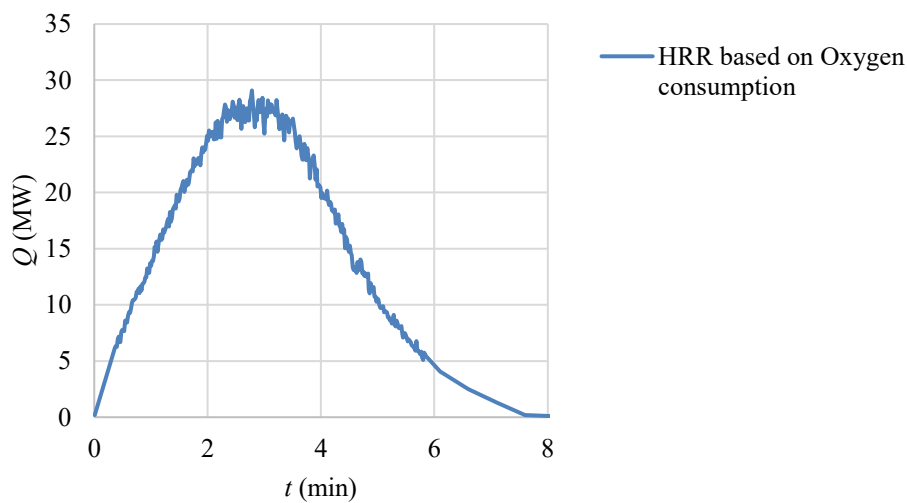


Figure 6 HRR curve for the calibration Test 2 with nominal HRR of 30 MW.

5.1.2 Smoke control

Test data concerning smoke control in tests 1 and 2 are presented in Table 4. In test 1, the smoke backlayering was located between 5 m and 15 m at the peak HRR period. An approximate estimate of the backlayering length was 10 m (average value). In test 2, the backlayering was located at around 50 m at peak HRR, and was quite stable. This was known from the temperature readings at 50 m and also from videos that were movable. For a period of at least 2 min, the backlayering was maintained between 45 m and 55 m. The minimum velocity referring to the backlayering length of 55 m in test 2 is given in Table 4. Both upstream and downstream velocities are shown. It was found that there exist some differences between the upstream velocity and downstream velocity after the fire starts (after correction due to heat and blockage), although prior to the ignition they are consistent. As shown in Table 4, in test 1, both upstream and downstream velocities are about 2.7 m/s. However, in test 2, the downstream velocity is slightly higher than the upstream value. This could be due to the hot gas expansion related to the larger fire size and partially to the measurement errors. As the critical velocity is defined as the minimum velocity to prevent backlayering, it was decided to refer to the upstream velocity instead of the downstream velocity, in case that there are differences between them.

From the observations of the tests and test data, the backlayering was relatively stable during at least 2.5 min. The two scenarios here could be considered as quasi-steady.

Table 4. Data concerning smoke control in tests 1 and 2.

| Test name | Initial velocity | HRR | $u_{o,us}$ | $u_{o,ds}$ | L_b | Note |
|-----------|------------------|-----|------------|------------|-------|------------|
| | m/s | MW | m/s | m/s | M | |
| Test 1 | 3 | 7.5 | 2.7 | 2.7 | ~10 | 5 m - 15 m |
| Test 2 | 2.6 | 28 | 2.15 | 2.3 | ~55 | ~ 55 m |

Figure 7 shows the critical velocities from the tests 1 and 2. The critical velocities are estimated using Eq. (2) with the aid of data for backlayering lengths and upstream velocities. The obtained critical velocities correlate well with Eq. (1). However, both test data lie above the line, indicating that the obtained critical velocities are slightly higher than the model predictions. There may be several reasons for this discrepancy. One possible factor is measurement accuracy, including the determination of correction factors, flow profiles, backlayering length and the estimation of blockage effects, which were not considered in the calculations. Additionally, differences between full-scale and model-scale experimental data may arise due to the limited availability of full-scale test results. However, previous comparisons have not shown significant deviations. This highlights the need for further full-scale testing to better understand these differences. The full-scale tests presented here consistently yield values that are higher, rather than lower, than those predicted by the model.

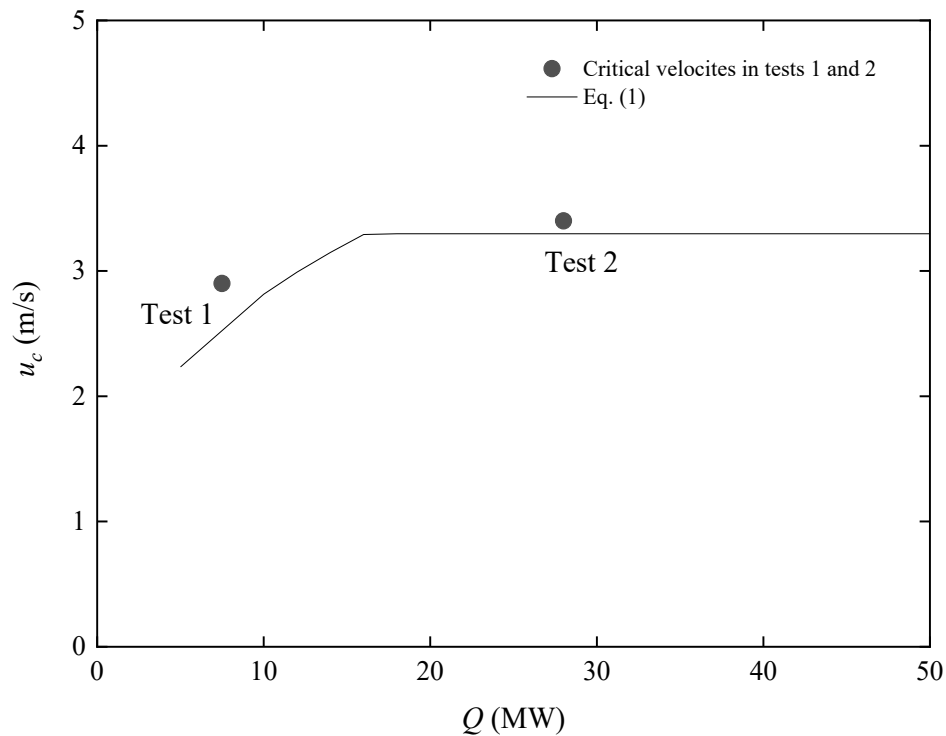


Figure 7. Comparison of measured and predicted critical velocity in tunnel.

5.2 Other tests prior to water spray activation

For the other tests, the heat release rate curves are similar to that for test 2, except the fact that the heat release rate is slightly higher than that due to the large pool area. In most of the tests, the HRR closely increases linearly to 30 – 40 MW within the first 2 min.

The tests are not quasi-steady, and the results are expected to have higher uncertainties than those from tests 1-2. The test data concerning smoke control in tests 3-12 are presented in Table 5.

Table 5. Data concerning smoke control in tests 3-12.

| Test name | Initial velocity | HRR | $u_{o,us}$ | Note on backlayering lengths |
|-----------|------------------|-----------|------------|------------------------------|
| | m/s | MW | m/s | |
| Test 3 | 2.5 | 35 | 1.8 | 50 m - 100 m |
| Test 4 | 1.4 | 40 | 1.2 | >100 m |
| Test 5 | 3 | 30.5 | 2.3 | 25 m - 50 m |
| Test 9 | 2.5 | 13 | 2.1 | 25 m - 50 m |
| Test 10 | 2.4 | 35 | 1.9 | 50 m - 100 m |

Figure 8 shows a comparison of the critical velocities from the tests 1 and 2 (solid rectangulars), and the results obtained from tests 3 – 12 as well as Eq. (1). In tests 3-12, it is either known that the smoke backlayering was controlled within a 25 m or 50 m long section or beyond 100 m. It is difficult to get a good estimate of the exact backlayering length. Therefore, the range where the critical velocities should lie is plotted instead with the aid of Eq. (2) (interval bar). In Figure 8, they are called controlled backlayering (referring to the upper limit for backlayering length) and uncontrolled backlayering (referring to the lower limit for backlayering length). For example, in

test 3, the backlayering length should lie between 50 m and 100 m. If 50 m is used to estimate a critical velocity, this critical velocity should be lower than the critical velocity referring to a backlayering length longer than 50 m. If 100 m is used to estimate a critical velocity, this critical velocity should be higher than the critical velocity referring to a backlayering length shorter than 50 m. By doing this, the range where the critical velocities should lie is obtained.

As shown in Figure 8, all the data for “Controlled backlayering” are above the line, and all the data for “Uncontrolled backlayering” are below the line. This provides additional support to Eq. (1), besides the solid data points that refer to critical velocity. Note that it is only known that the critical velocity should lie between the two data sets, or beyond the data point. The ranges are shown using dash lines in this figure.

It should, however, be noted that the data correspond to the first 2 minutes of the tests (prior to activation of water spray system). Both the fire and the flow are highly transient and therefore the scenarios can not be regarded as quasi-steady. It is usually believed true that, for a given velocity, if the test was prolonged, the backlayering length would be slightly longer.

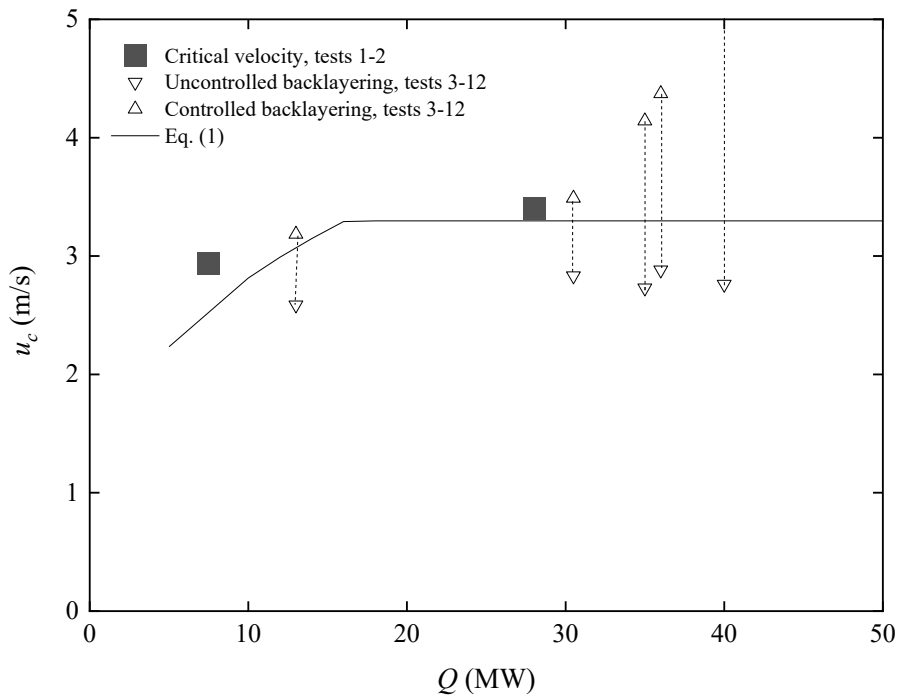


Figure 8. Comparison of measured and predicted critical velocity based on upstream velocity.

As mentioned previously, there are some differences between the upstream velocities and the downstream velocities to see how large the difference could be. The reason has been explained earlier. In this section, we analyze the results using the downstream velocities instead. The results are shown in Figure 9. The data were treated in the same way as in Figure 8. The critical velocities from tests 1 and 2 (the solid points) are similar to those in Figure 8 but for test 2 with 28 MW fire, the estimated critical velocity is slightly higher. This could be attributed to either the transient behavior of the fire and smoke or the measurement errors. Overall, the differences between the upstream and downstream velocities are small for tests 1-2 which contain a quasi-steady state burning period (at least 2.5 min).

For tests 3 – 12, the estimated range where the critical velocity should lie is also slightly higher than that in Figure 8, and Eq. (1) is either at the lower limit of the range or within the range.

Overall, the differences between the upstream and downstream velocities are more significant for these tests with varying heat release rates within 2 min after ignition. It is recommended that tests should be designed to be quasi-steady to obtain high-quality data.

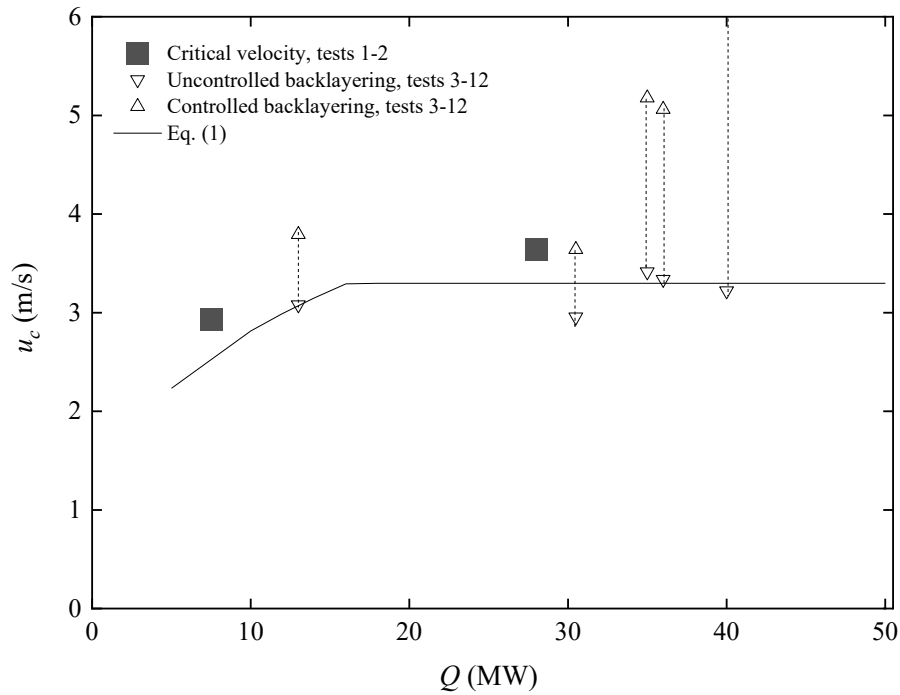


Figure 9. Comparison of measured and predicted critical velocity based on downstream velocity.

6 Conclusion

Data from two free-burn tests were analyzed, as well as data from the first 2 mins of five other tests. Different diesel pools were used as the fire sources.

The data from the free-burn tests are relatively stable, and produce strong support for the previous prediction models. The differences between the upstream velocities and downstream velocities are small. The data are compared with the established prediction model and show good consistency.

The other five tests were designed to test the performance of a water mist system so only the data prior to its activation were analyzed. Both the fire and the flow are transient. The scenarios are not quasi-steady, which is usually used when determining the critical velocity. It is generally believed to be true that, for a given velocity, if the test was prolonged, the backlayering length would be slightly longer due to heating of walls and stabilization of the fire source. Furthermore, the differences between the upstream velocities and downstream velocities are more significant. This could be attributed to the transient behaviour of fire and smoke (hot gas expansion related to the larger fire size) and partially to the measurement errors. It is recommended that tests should be designed to be quasi-steady to obtain high-quality data in order to compare with Eqs. (1) and (2).

The blockage ratio close to the upstream edge of the fire source is within 4% - 5%. The blockage ratio from the upstream edge of the fire source to 25 m upstream is about 2%. For the further upstream section of interest to this study, the blockage is negligible. Overall, the influences of these upstream blockages are considered small and the data for smoke control have not been corrected using the upstream blockage ratios. If corrections using upstream blockage ratios were done, the data would be slightly higher. Furthermore, the tunnel surfaces near the fire are covered with sprayed concrete, but they remain relatively rough. This roughness might influence the backlayering and critical velocity. If the tests were carried out in a smooth tunnel, the data would be slightly higher. However, this effect is generally considered minor or negligible, particularly when the backlayering length is short.

References

1. Li, Y.Z., B. Lei, and H. Ingason, *Study of critical velocity and backlayering length in longitudinally ventilated tunnel fires*. Fire Safety Journal, 2010. **45**: p. 361-370.
2. Li, Y.Z. and H. Ingason, *Effect of cross section on critical velocity in longitudinally ventilated tunnel fires*. Fire Safety Journal, 2017. **91**: p. 303–311.
3. Li, Y.Z. and H. Ingason, *Influence of upstream blockage on smoke control in tunnel fires*. Fire Safety Journal, 2024. **147**: p. 104197.
4. Gannouni, S. and R.B. Maad, *Numerical study of the effect of blockage on critical velocity and backlayering length in longitudinally ventilated tunnel fires*. Tunnelling and Underground Space Technology, 2015. **48**: p. 147-155.
5. Hong, Y., J. Kang, and C. Fu, *Rapid prediction of mine tunnel fire smoke movement with machine learning and supercomputing techniques*. Fire Safety Journal, 2022. **127**: p. 103492.
6. Weng, M.-c., X.-l. Lu, F. Liu, X.-p. Shi, and L.-x. Yu, *Prediction of backlayering length and critical velocity in metro tunnel fires*. Tunnelling and Underground Space Technology, 2015. **47**: p. 64-72.
7. Weng, M.-c., X.-l. Lu, F. Liu, and C.-x. Du, *Study on the critical velocity in a sloping tunnel fire under longitudinal ventilation*. Applied Thermal Engineering, 2016. **94**: p. 422-434.
8. Zhang, T., G. Wang, J. Li, Y. Huang, K. Zhu, and K. Wu, *Experimental study of back-layering length and critical velocity in longitudinally ventilated tunnel fire with various rectangular cross-sections*. Fire Safety Journal, 2021. **126**: p. 103483.
9. Janssens, M.L., *Measuring Rate of Heat Release by Oxygen Consumption*. Fire Technology, 1991: p. 234-249.
10. Li, Y.Z., B. Lei, and H. Ingason, *The maximum temperature of buoyancy-driven smoke flow beneath the ceiling in tunnel fires*. Fire Safety Journal, 2011. **46**(4): p. 204-210.
11. Li, Y.Z. and H. Ingason, *The maximum ceiling gas temperature in a large tunnel fire*. Fire Safety Journal, 2012. **48**: p. 38-48.

Appendix – Measurements at different cross sections

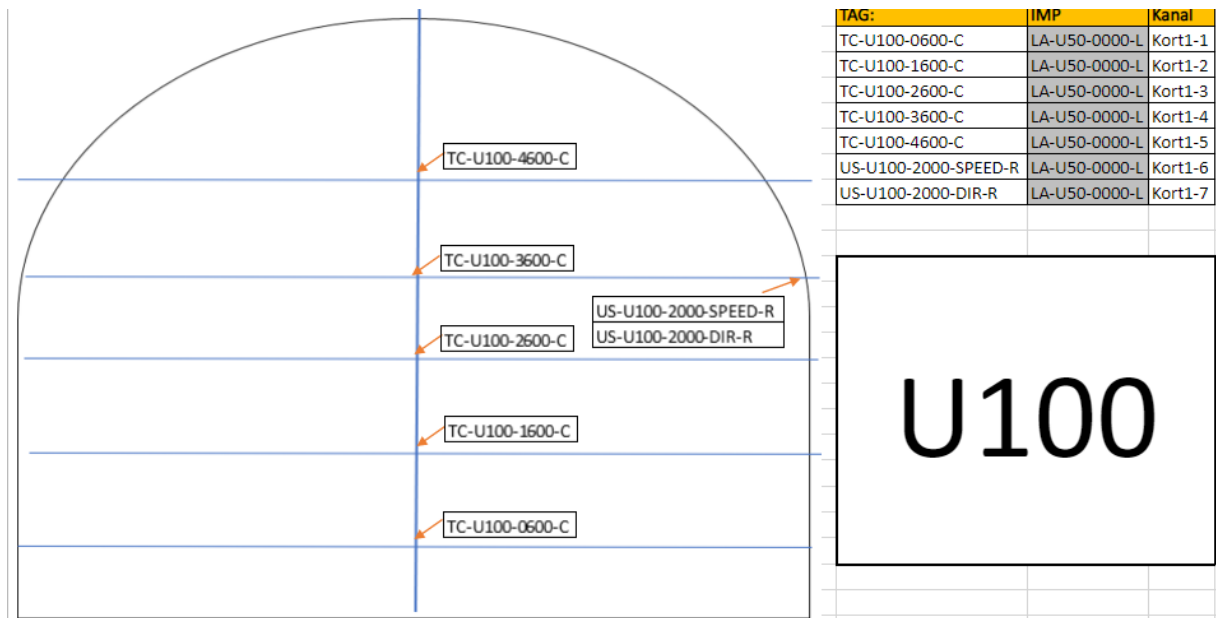


Figure 0-1 Measurements 100 m upstream (U100).

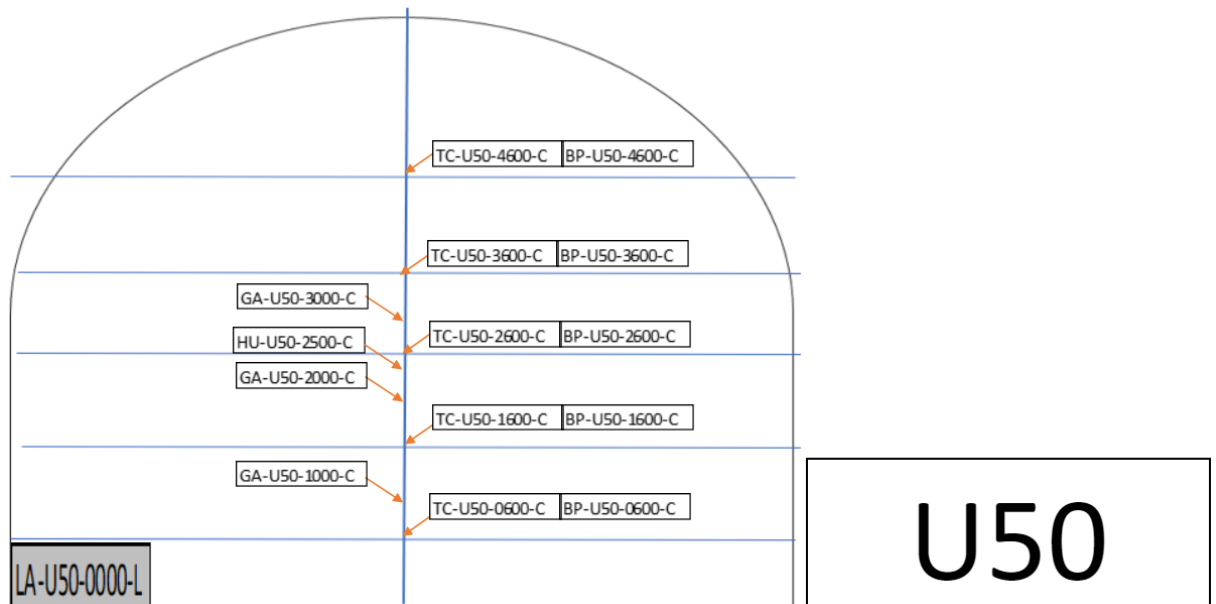


Figure 0-2 Measurement 50 m upstream (U50).

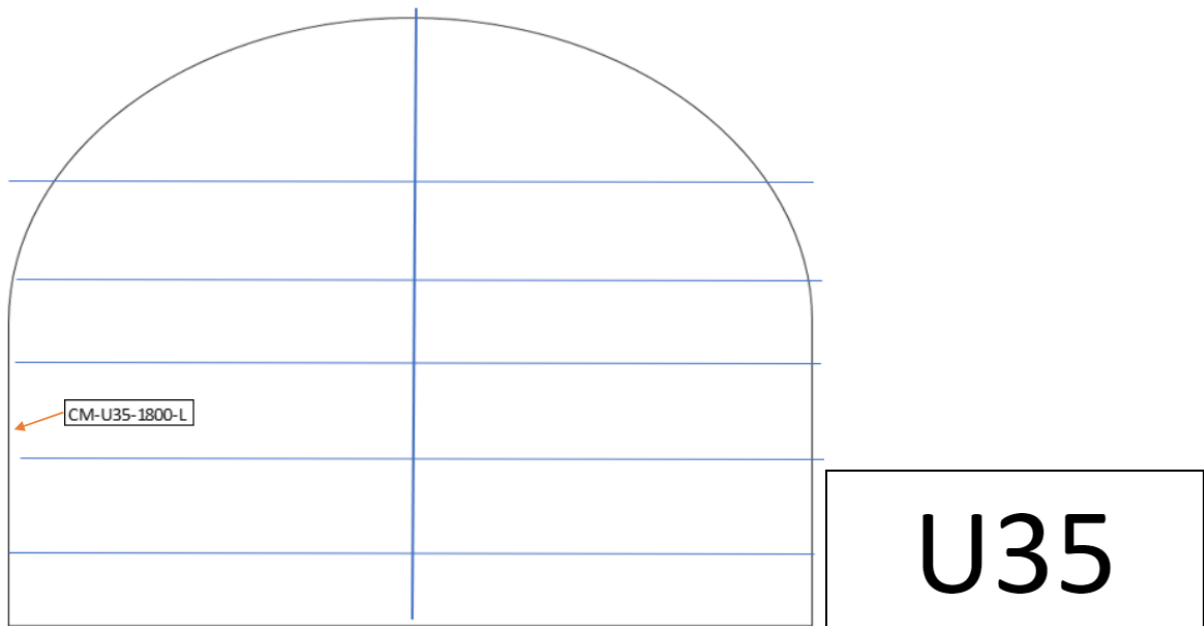


Figure 0-3 Measurement 35 m upstream (U100).

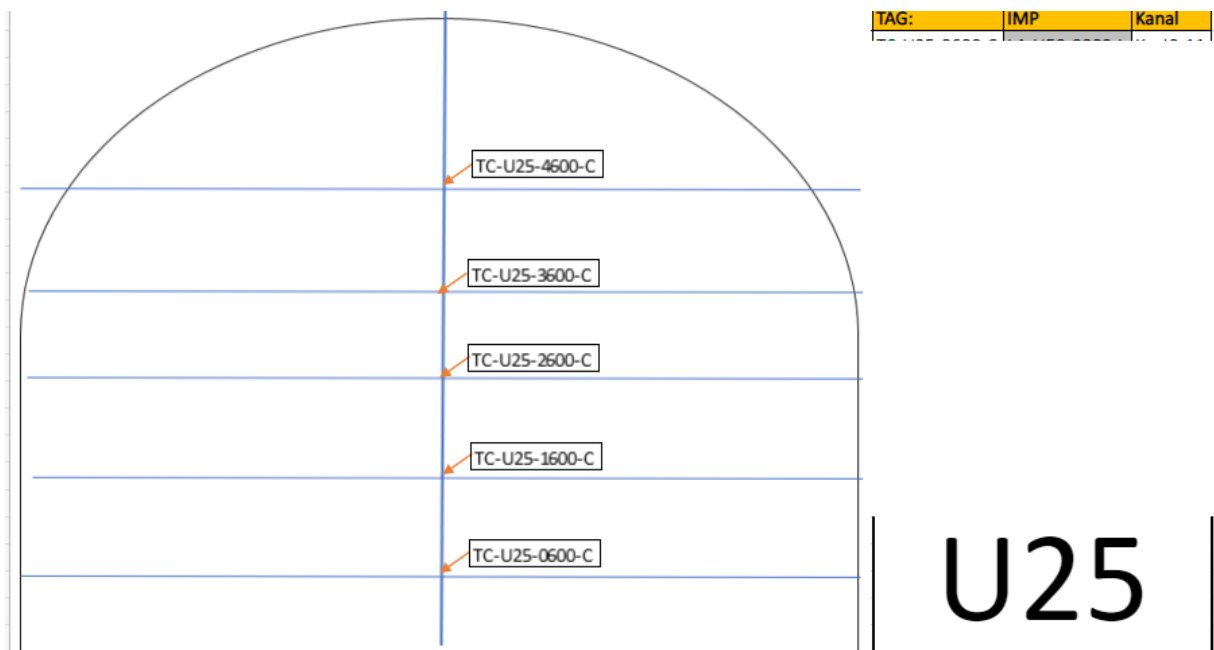


Figure 0-4 Measurement 25 m upstream (U25).

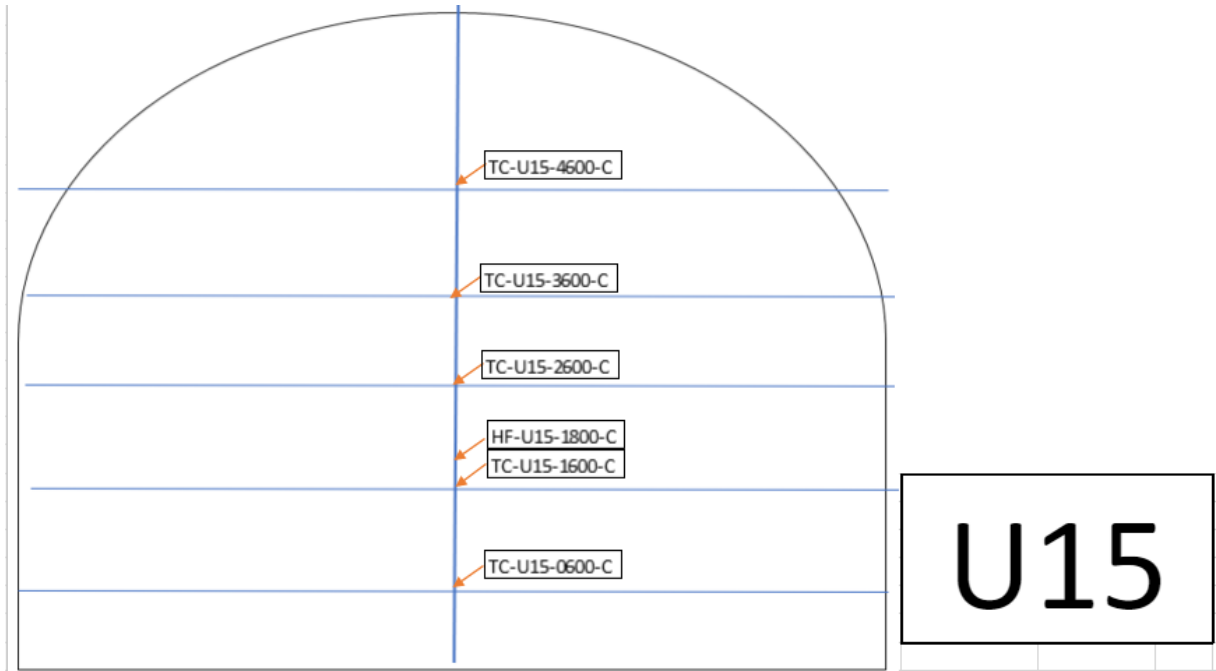


Figure 0-5 Measurement 15 m upstream (U15).

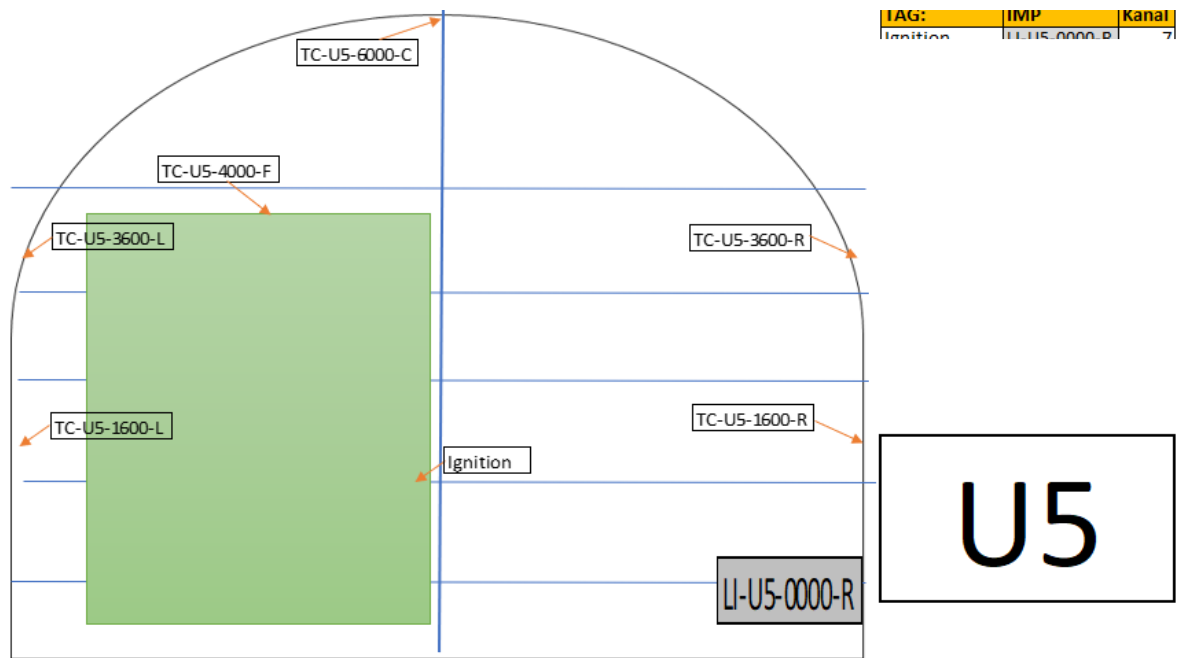


Figure 0-6 Measurement 5 m upstream (U5).

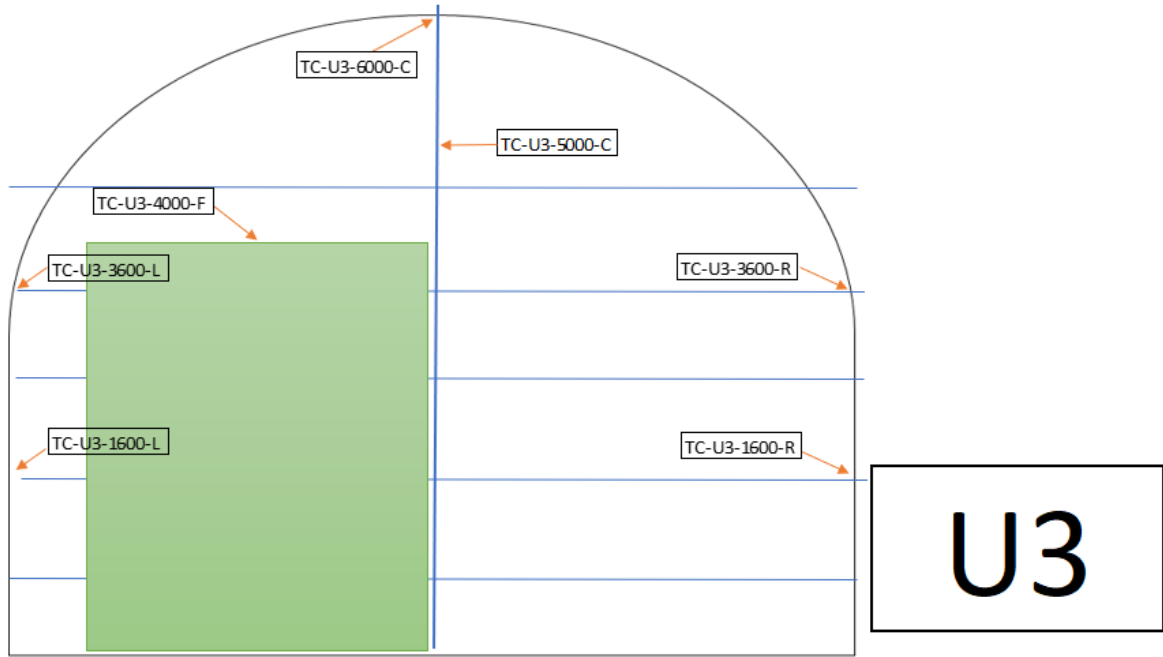


Figure 0-7 Measurement 3 m upstream (U3).

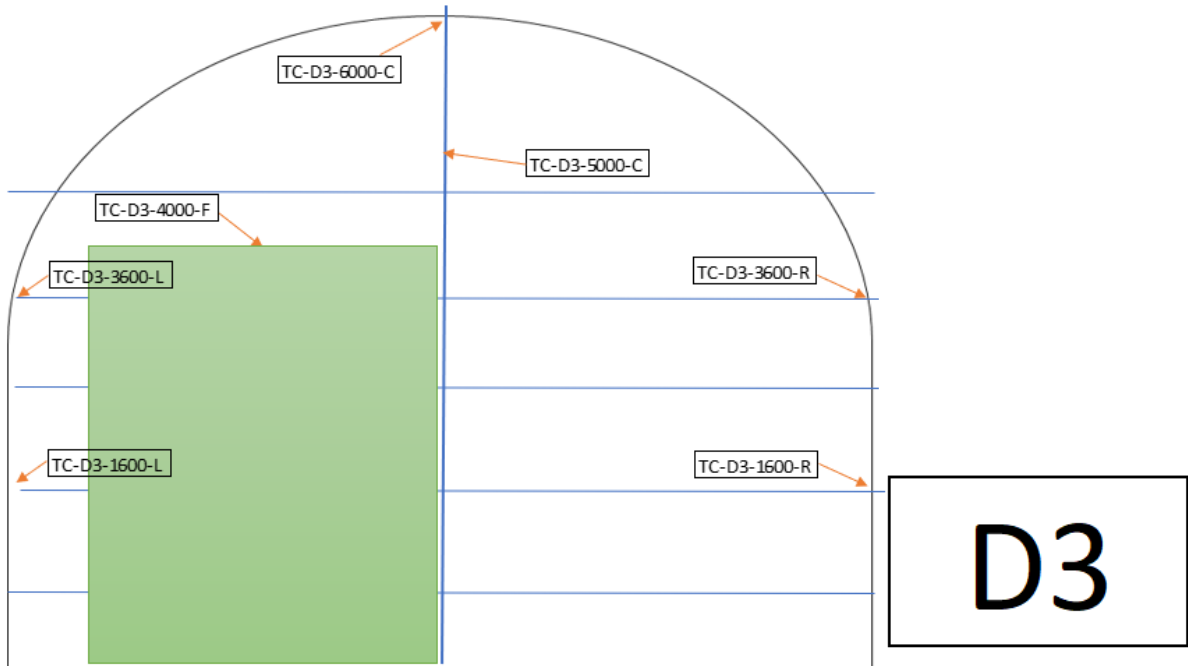


Figure 0-8 Measurement 3 m downstream (D3).

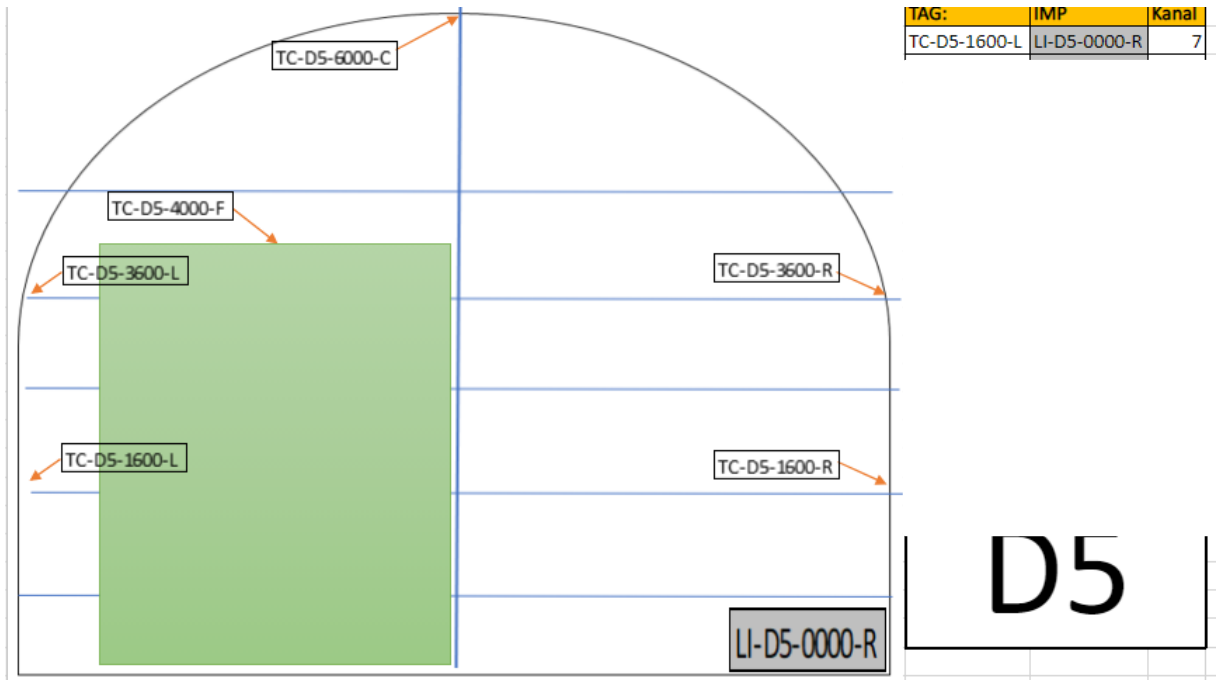


Figure 0-9 Measurement 5 m downstream (D5).

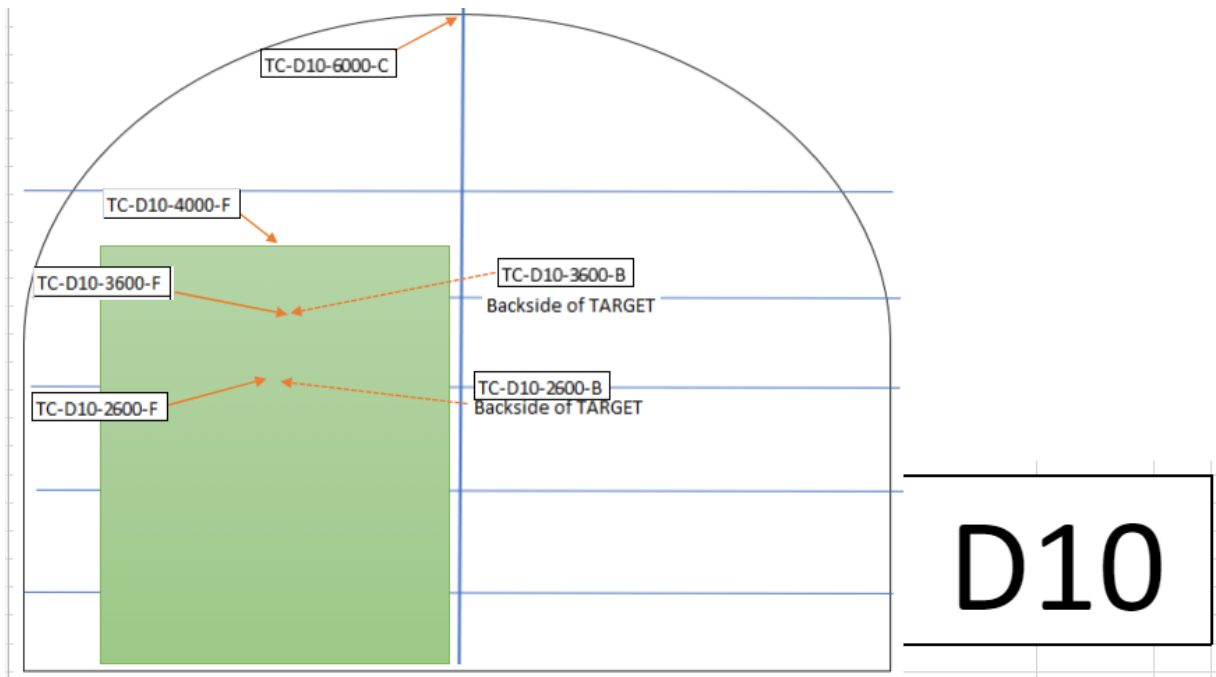


Figure 0-10 Measurement 10 m downstream (D10).

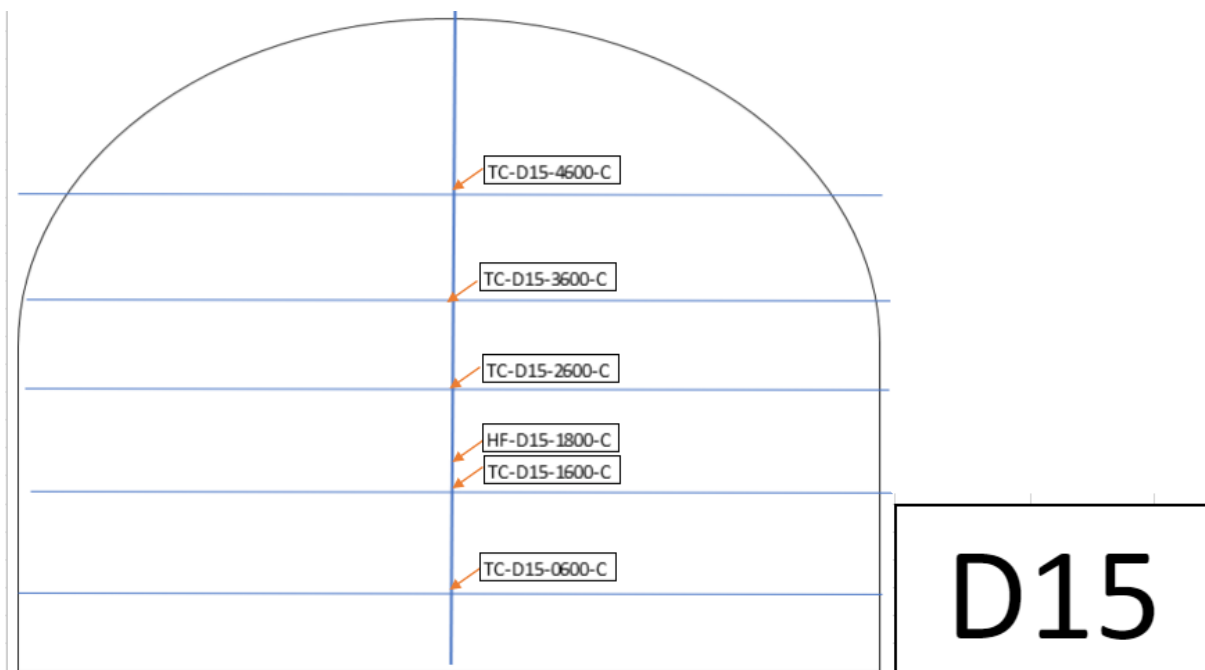


Figure 0-11 Measurement 15 m downstream (D15).

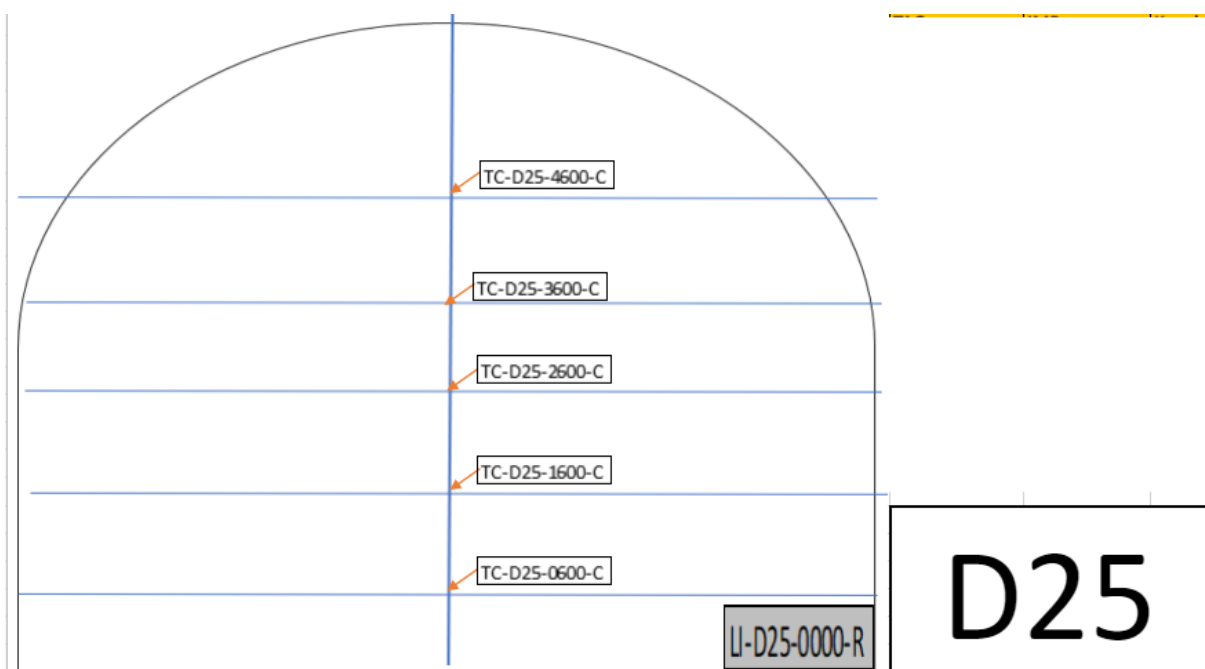


Figure 0-12 Measurement 25 m downstream (D25).

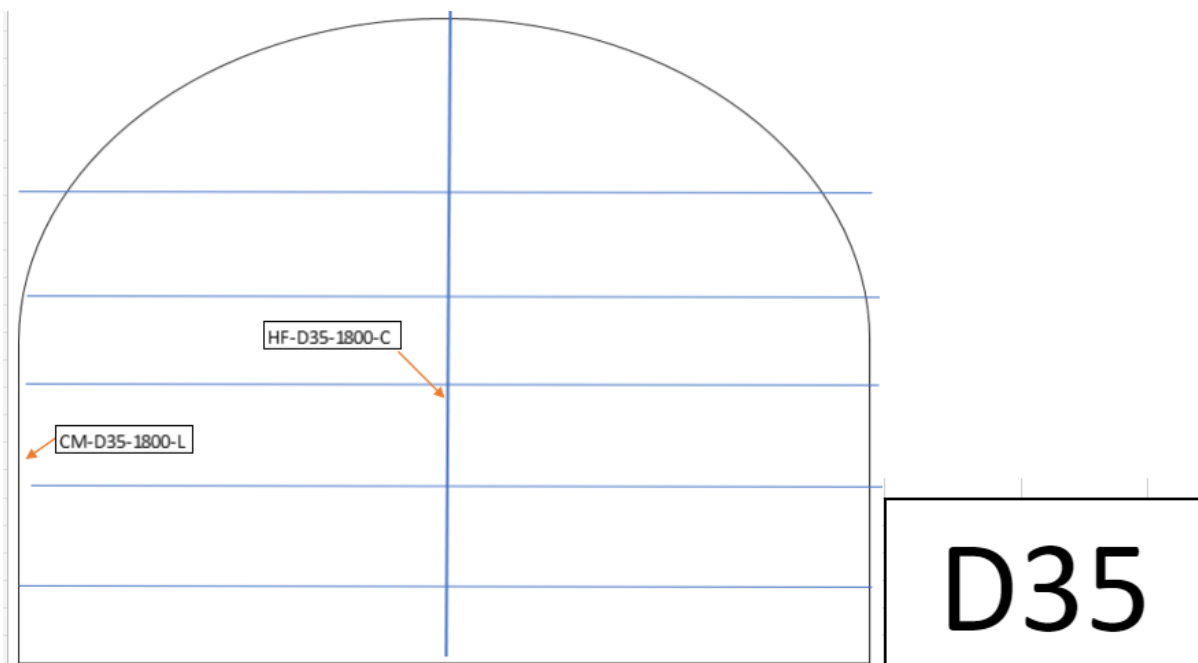


Figure 0-13 Measurement 35 m downstream (D35).

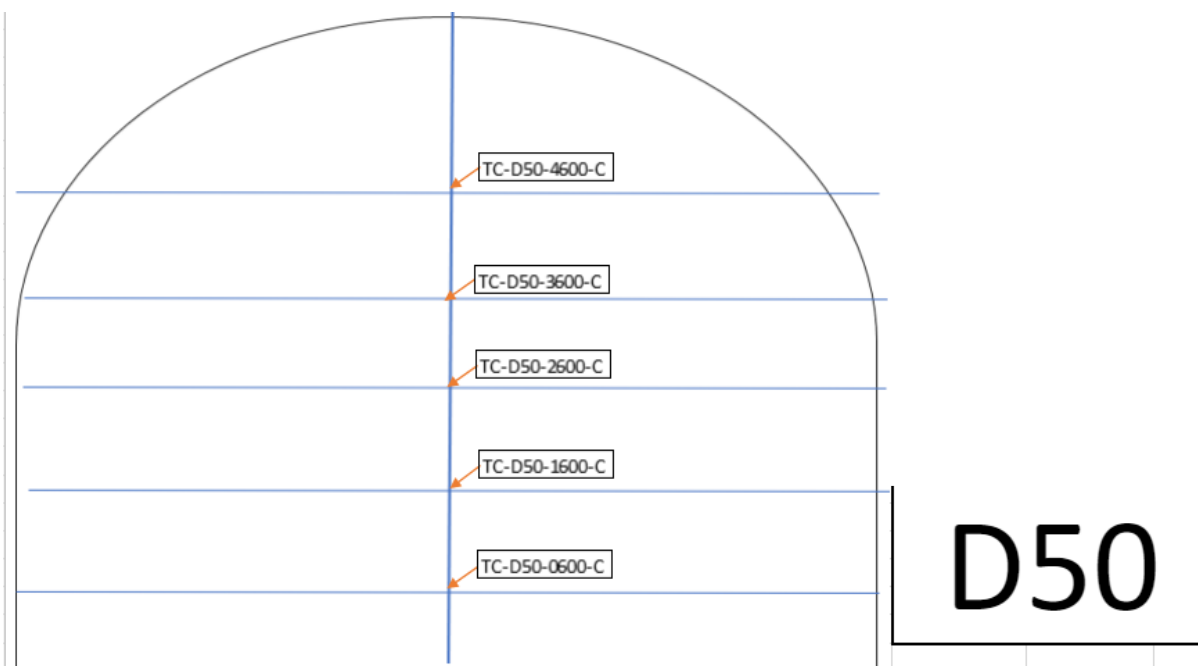


Figure 0-14 Measurement 50 m downstream (D50).

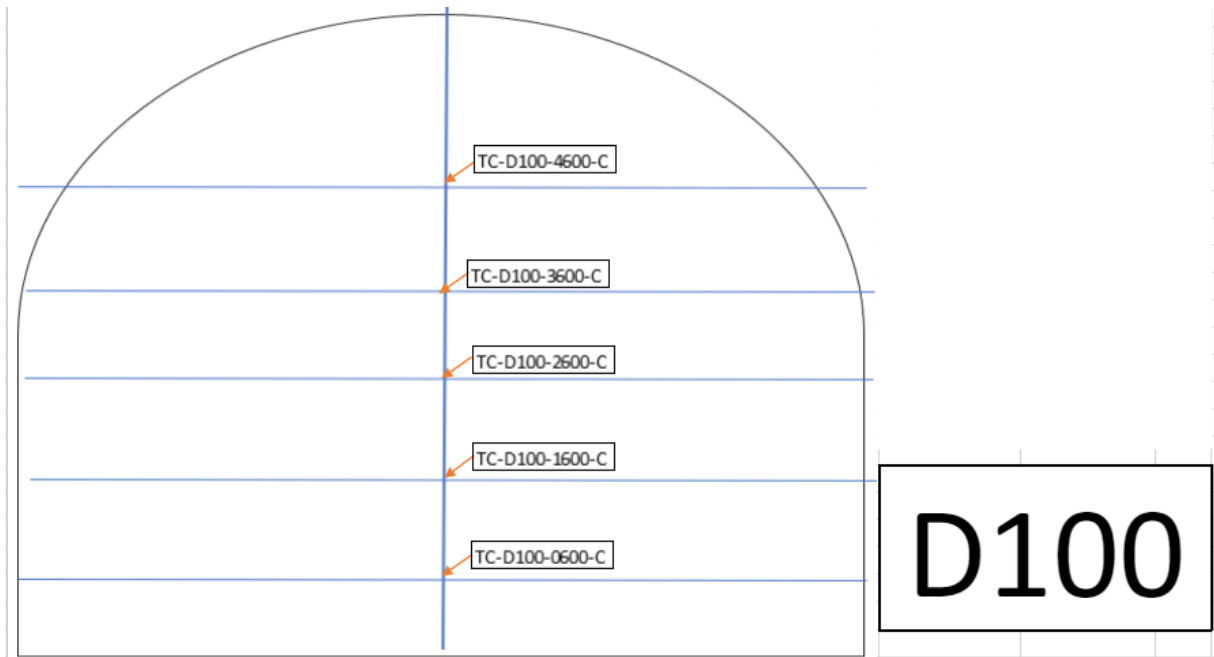


Figure 0-15 Measurement 100 m downstream (D100).

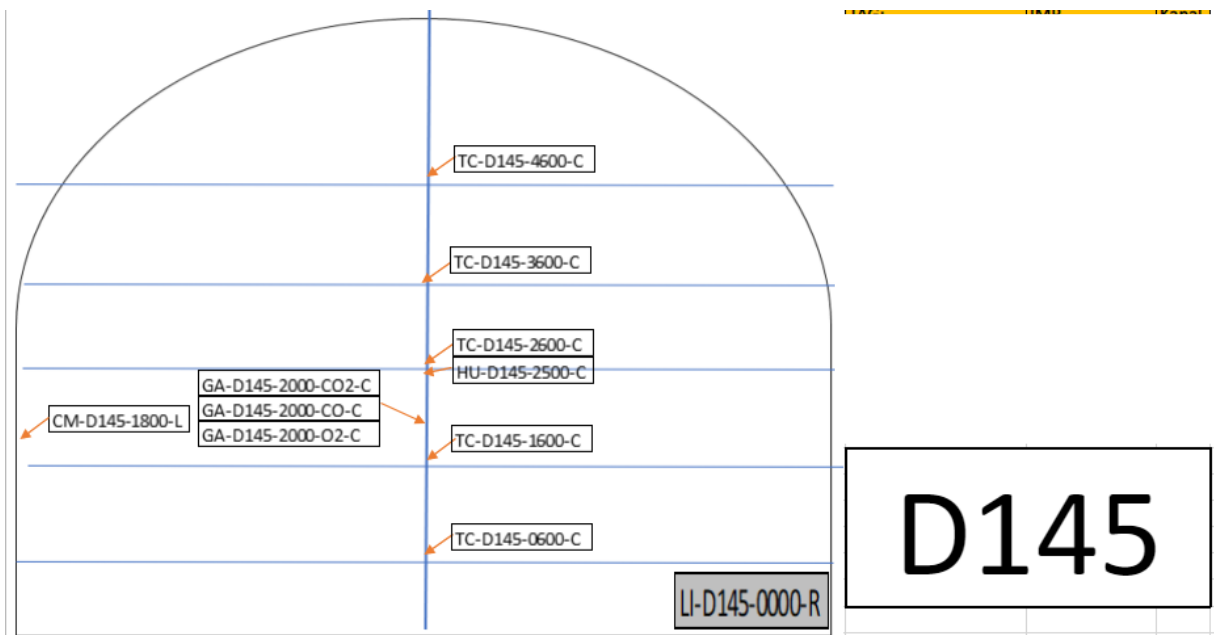


Figure 0-16 Measurement 145 m downstream (D145).

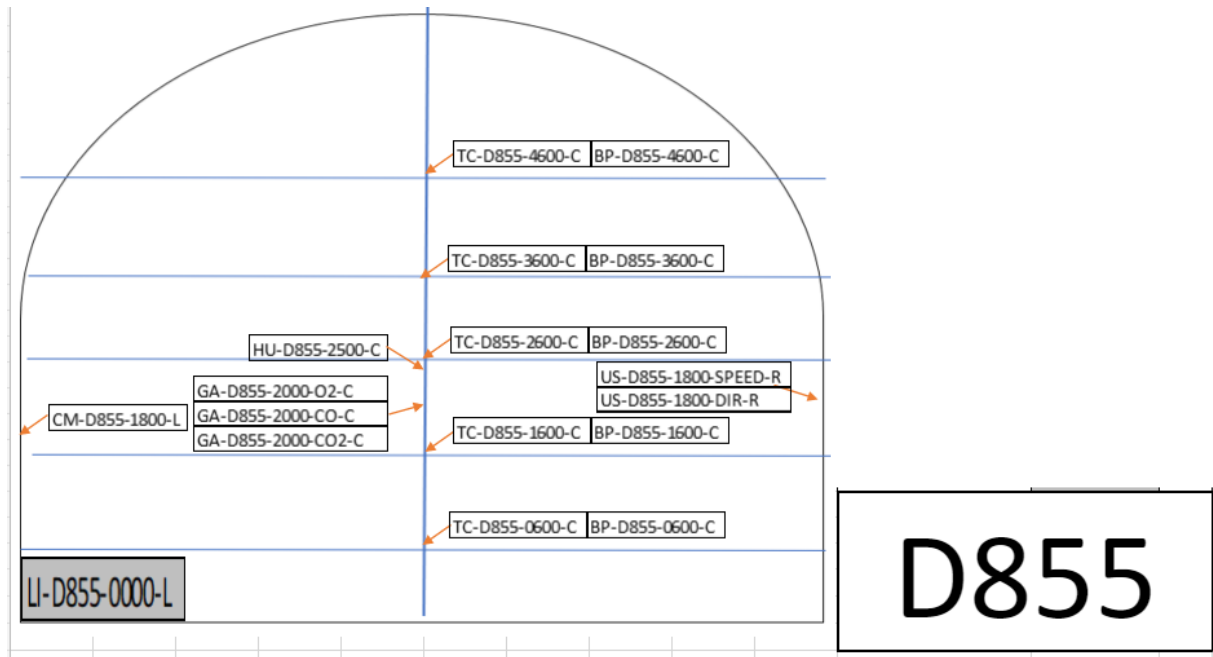


Figure 0-17 Measurement 855 m downstream (D855).